Journal of Membrane Science 546 (2018) 234–245

Contents lists available at ScienceDirect

Journal of Membrane Science

journal homepage: www.elsevier.com/locate/memsci

Water and salt transport properties of disulfonated poly(arylene ether sulfone) desalination membranes formed by solvent-free melt extrusion

Hee Jeung Oh[a], James E. McGrath[b,1], Donald R. Paul[a,*]

[a] The University of Texas at Austin, McKetta Department of Chemical Engineering, 1 University Station, Mail Code: C0400, Austin, TX 78712, USA
[b] Virginia Polytechnic Institute and State University, Department of Chemistry, Blacksburg, VA 24061, USA

ARTICLE INFO

Keywords:
Sulfonated polysulfone
Poly(ethylene glycol)
Melt extrusion
Desalination
Transport property

ABSTRACT

This paper reports water and salt transport properties of sulfonated polysulfone desalination membranes prepared by solvent-free, melt extrusion. The 20 mol% disulfonated poly(arylene ether sulfone) (BPS-20K) membranes were prepared by melt processing, using poly(ethyelene glycol) (PEG) $\overline{M}_n$ (200 ~ 400 g/mol) as plasticizers at concentrations of 20 wt% to 30 wt%, and different PEG extraction temperatures. Water and salt transport properties of BPS-20K membranes prepared by different processing routes correlated well with water uptake, as expected, based on free volume theory. The melt-extruded BPS-20K membranes show higher water uptake than those of solution cast membranes. As PEG molecular weight and concentration used during extrusion increases and as PEG extraction temperature increases, water uptake also increases. As water uptake increases, water and salt permeabilities and diffusivities increase, consistent with the findings of Yasuda *et al.* In general, BPS-20K membranes prepared by different processing routes followed the trade-off relationship between water permeability and water/salt permeability selectivity. These results indicate that differences in membrane processing history have significant effects on the transport properties of small molecules in these polymers, similar to other glassy polymers.

1. Introduction

Many ionomer membranes used for water purification [1–4] and electricity generation [5,6] are produced by solution processing methods. Because solution processing consumes large amounts of biologically toxic and hazardous solvents, the preparation process is environmentally unfriendly, and the cost related to waste disposal is high. There is, consequently, a great need to prepare ionomer membranes by more environmentally friendly methods, without the use of hazardous solvents.

Sulfonated polysulfones have been explored as candidate materials for reverse osmosis desalination [4,7–10] and fuel cell applications [6,11–15], thanks to their good selective ion transport properties and their strong thermal and mechanical stabilities [4,6–15]. Moreover, sulfonated polysulfone membranes may be produced without using solvent—i.e., by melt extrusion—with the aid of adequate plasticizers, such as poly(ethylene glycol) [16,17]. Because of the influence of sulfonic groups on the polysulfone polymer matrix, the glass transition temperatures (T_g) of sulfonated polysulfone are high, and thus, in general, the melt processing of such polymers is challenging [17,18]. However, an appropriate plasticizer, i.e., poly(ethylene glycol) (PEG) materials, can sufficiently alter the T_g and viscosity of sulfonated polysulfone to make the extrusion process successful [16,17]. This plasticizer can then be eliminated from the extruded membranes with water extraction. In this study, we examine this new path to producing sulfonated polysulfone membranes for use in desalination.

Earlier, Bebin *et al.* reported some properties of post-sulfonated polysulfone membranes prepared by extrusion for proton exchange membrane fuel cell (PEMFC) applications [19,20]. They measured the proton conductivity, as well as the life span of extruded membranes, and compared the values to those of solution cast membranes. The extruded membranes were reported to have lower proton conductivity but longer life span than did solution cast membranes. Similarly, Sanchez et al. used the post-sulfonated polysulfones and extruded membranes for PEMFC applications [21–25]. They reported the influence of various plasticizers on the thermal and rheological properties. These studies focused on fuel cell applications; there has been no investigation regarding the use of melt extrusion for preparing desalination membranes.

For desalination applications, thin film composite membrane structures ultimately would need to be prepared via a coextrusion process using the appropriate supporting materials [26–28]. Thin film

* Corresponding author.
E-mail address: drp@che.utexas.edu (D.R. Paul).
[1] Deceased.

https://doi.org/10.1016/j.memsci.2017.09.070
Received 17 August 2016; Received in revised form 15 September 2017; Accepted 23 September 2017
Available online 28 September 2017
0376-7388/

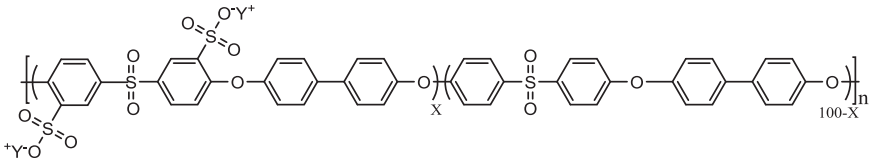

Fig. 1. Chemical structure of disulfonated poly(arylene ether sulfone) random copolymer (BPS-XY). X = mol% of disulfonated monomer (0 < X < 100), Y = H (acid form) or K (potassium salt form).

composite structures are composed of a thin, selective layer (sulfonated polysulfone in this project) and a support layer with desirable porosity. The thin, selective layer provides high selectivity of ions (i.e., high salt rejection), while the porous support layer gives strong mechanical stability, while also preserving high water flux [2,29]. In this project, polypropylene (PP) can serve as a candidate material for the porous support layer in thin film composite structures because its porosity level can be controlled in numerous ways, including stretching after coextrusion [26,30,31].

In this work, disulfonated poly(arylene ether sulfone)s (BPS) have been investigated for desalination membrane application, and poly (ethylene glycol) (PEG) materials have been chosen as plasticizers for preparing thin, single layer membranes of BPS by melt extrusion. Previously, we reported the effect of several PEG materials on the T_g and viscosity of BPS/PEG blends and identified the formulations of BPS/PEG blends that were rheologically compatible with PP to enable formation of the composite structures [16,17]. Single layer, uniform thickness membranes of BPS-20K/PEG blends were prepared by melt extrusion [32], and PEG materials were successfully removed by water extraction from the extruded BPS/PEG membranes before their use as membranes [33]. Factors affecting the PEG diffusion from the extruded films were explored experimentally and theoretically to elucidate this membrane preparation path [33,34].

Consequently, this paper reports water and salt transport properties of disulfonated poly(arylene ether sulfone) (BPS) membranes prepared by melt extrusion. The extruded BPS membranes were prepared using PEG plasticizers with $\overline{M}_n$ ranging from 200 g/mol to 400 g/mol and concentrations of 20 wt% to 30 wt% during extrusion. PEG extraction temperatures were varied. Water and salt transport properties, including salt solubility, diffusivity, permeability, water uptake, diffusivity, and permeability of melt-extruded films, were measured. The results were then compared to the properties of solution cast membranes in order to help us understand the effects of different preparation routes on the transport properties of small molecules in BPS materials. Free volume theory was used to interpret the results.

Furthermore, one objective of the current study was to more completely understand how varying the processing method might provide extra freedom to modify the polymer transport properties, in addition to varying the chemical structure of the polymer. Previously, Park *et al.* studied a series of sulfonated polysulfones similar to those studied in this work and investigated the influence of varying the chemical structure of these polymers—with a specific processing history—on the transport properties [7,8,10]. When they studied the effect of the sulfonation level (20–40 mol%) and ionic forms (K or H forms) of the polymers on the water and salt transport properties for desalination applications, they found that both the sulfonation level and ionic forms greatly influenced the polymers' transport properties. The polymers with increased sulfonation levels and in the acid (H) form showed increased hydrophilicity, as indicated by higher water uptake, and, thus, exhibited increased water and salt diffusivity and permeability.

On the other hand, Xie et al. used one sulfonated polysulfone (i.e., BPS-32K) with a fixed chemical structure in terms of the sulfonation level (32 mol%) and ionic form (K form) from polymerization and reported the influence of processing history on water and salt transport properties of solution cast BPS-32K polymers [4]. The BPS-32K polymers conditioned via acid treatment, thermal treatment, ion-exchange, and solution and solid state acidifications exhibited a broad range of transport properties, indicating that different processing routes could be further used to tune the transport properties of BPS polymers. They proposed that these properties are sensitive to processing history because the glassy BPS polymers would be in a non-equilibrium state below their T_g. Other glassy polymers, such as perfluorinated sulfonated polymers (Nafion®), also have been reported to be strongly influenced by their processing history. The influence of processing history on electro-transport properties, water uptake, and hydraulic permeabilities was reported for Nafion membranes, and these effects were correlated with morphological rearrangement [35–37]. With this perspective, we started with one polymer, BPS-20K, and studied the influence of different processing routes (i.e., melt processing) on transport properties. We wished to place the water and salt transport properties found in this study in context, comparing them with the effects of varying the chemical structures of polymers with fixed processing routes.

2. Materials and experiments

2.1. Materials

2.1.1. Polymer: 20 mol% disulfonated poly(arylene ether sulfone) (BPS-20K)

Disulfonated poly(arylene ether sulfone) random copolymers (BPS-XY), shown in Fig. 1, were synthesized from sulfonated monomers following procedures established by McGrath and others [7–10,38]. In the nomenclature for this polymer, BPS-XY, X represents the mol% of hydrophilic sulfonated groups and Y denotes the cation types, such as K (potassium form) or H (free acid form). For instance, BPS-20K contains 20 mol% sulfonated sulfone monomers and 80 mol% of non-sulfonated sulfone monomers in the K (potassium) sulfonated form.

In this study, the 20 mol% disulfonated poly(arylene ether sulfone) random copolymer, BPS-20K (ion exchange capacity (IEC) = 0.92 meq/g), was prepared by Akron Polymer Systems (Akron, OH) and used as received. BPS-20K was chosen because of its good selective ion transport properties and thermal and mechanical stabilities, as reported previously [7,8,10,17]. Several fundamental properties of BPS-20K polymer are presented in Table 1.

2.1.2. Plasticizer: poly(ethylene glycol) 200 ~ 400 g/mol

Poly(ethylene glycol) (PEG) materials were selected as plasticizers for the BPS polymer. PEG molecular weight ($\overline{M}_n$) 200 g/mol and 400 g/mol were used, and the PEG concentration (wt%) in the extruded membranes was changed from 20 wt% to 30 wt% to prepare thin membranes of uniform thickness. The PEG materials (PEG 200 Cat#

Table 1
Characteristics of the BPS polymer used in this study.

Material	$\overline{M}_w$[a] [g/mol]	IV[a] [ml/g]	T_g[b,d] [°C]	Density[c,d] [g/cm^3]
BPS-20K	29,700	41.7	256	1.35

[a] Determined by SEC using NMP with 0.05 M LiBr at 50 °C. Specific refractive index increment (dn/dc) values were measured using an assumption of 100% mass recovery. dn/dc values for BPS-20K polymers in this study are 0.17 [ml/g]. IV is intrinsic viscosity.
[b] Measured by DSC at 20 °C/min.
[c] Measured with *n*-heptane at ambient temperature (20–22 °C) using a Mettler Toledo density determination kit (Part# 238490, Switzerland).
[d] Measurements were conducted using solution cast films.

P3015 and PEG 400 Cat# 202398) were purchased from Sigma Aldrich (St. Louis, MO) and used as received.

2.2. Film preparation

2.2.1. Melt extrusion

Thin, single layer films of BPS-20K/PEG blends were produced by using a 5 ml twin screw micro-compounder with a connected heated film die (width = 65 mm) and film take-up system (DSM Xplore, The Netherlands). Processing temperatures were selected to be lower than the polymer degradation temperature, T_d, and 50 ~ 100 °C higher than the T_g of BPS/PEG blends. Depending on the blend compositions, the processing temperature was in the range of 225–240 °C. The processing temperatures of the samples are: 1) BPS-20K/PEG 200 g/mol 20 wt% : 230–240 °C; 2) BPS-20K/PEG 400 g/mol 20 wt% : 230–240 °C; and 3) BPS-20K/PEG 200 g/mol 30 wt% : 225–235 °C. BPS and PEG materials were well-mixed before being fed to the compounder and were melt-extruded under an extra dry nitrogen atmosphere (99.9%, Matheson Tri-Gas, Austin, TX) to prevent degradation. The speed and torque of the film take-up system were adjusted to prepare films of uniform thickness (20–50 μm). More details about the processing conditions have appeared previously [16,17,34].

PEG materials were extracted from extruded BPS-20K/PEG films using DI water (Millipore MilliQ system, Darmstadt, Germany) at three different temperatures (23 °C, 50 °C and 75 °C) for different times. Details of the PEG extraction process can be found in our previously published work [33,34].

2.2.2. Solution casting method

Dense, freestanding films of uniform thickness (30–50 μm) of BPS-20K polymer were prepared by using a solution casting method. BPS-20K was dissolved in N,N-dimethylacetamide (DMAc, Sigma Aldrich, Cat# 39940) and a 10 wt% polymer solution was prepared. This well-mixed solution was cast onto a glass plate and dried first in an oven for 24 h at 60 °C, then in a vacuum oven at 120 °C for 48 h to eliminate the DMAc solvent [4,8,10]. The film was subsequently immersed in deionized (DI) water for 24 h to extract residual solvent [8].

2.3. Polymer characterization

2.3.1. Differential scanning calorimetry (DSC)

DSC (Q100, TA Instruments, New Castle, DE) was used to measure the glass transition temperature, T_g. For each measurement, a 5 mg sample was placed in an aluminum pan, and DSC scans were recorded using a heating rate of 20 °C/min over the temperature range from −90 °C to 350 °C under ultra-high purity nitrogen (UHP 99.999%, Air Gas, Austin, TX). The T_g was taken as the midpoint of the heat capacity step change during the third (and final) heat cycle.

2.3.2. Fourier Transform Infrared Spectroscopy (FT-IR)

Attenuated Total Reflection (ATR) FT-IR (Nicolet 6700 FT-IR Spectrometer, Thermo Scientific, Waltham, MA) was used to examine the chemical structural changes in BPS-20K films prepared by different processing paths. For each sample, 64 spectra were collected in air at a resolution of 4 cm^{-1}.

2.4. Transport property characterization

2.4.1. Estimation of P_w, K_w, and D_w

The water uptake (i.e., g water/g dried polymer, ω_W) of the polymer membrane was determined from the mass of a dried sample (m_d) and the mass of a hydrated sample (m_h) as follows [4,8]:

$$\omega_W = \frac{m_h - m_d}{m_d} \times 100[\%] \tag{1}$$

For water uptake measurements, membrane samples of similar size (circular coupon, D = 2.5 cm) were soaked in ultrapure deionized water (using Millipore MilliQ system) at ambient temperature for 48 h. Before weighing the sample, we carefully removed excess water on the sample surface with tissue paper. The hydrated sample mass, m_h, was measured periodically to ensure that a constant hydrated mass was reached. Next, the samples were dried in a vacuum oven at 110 °C for at least 48 h before measuring their dry mass, m_d. The sample mass was measured occasionally to ensure that a constant dry mass was reached [4,8].

The equilibrium volume fraction of water of the hydrated polymer membrane (ϕ_W) was calculated by assuming ideal mixing behavior and volume additivity of water with the polymer membrane:

$$\phi_W = \frac{(m_h - m_d)/\rho_W}{(m_h - m_d)/\rho_W + m_d/\rho_P} \tag{2}$$

where ρ_W is the water density (1.0 g/cm^3 is used) and ρ_P is the density of the dry polymer membrane.

The water solubility (i.e., water partition coefficient or water sorption coefficient, K_W) is the ratio of water concentration in the polymer membrane (C_W^m) to the water concentration of the external solution (C_W) [4,8,39].

$$K_W = \frac{C_W^m}{C_W}\left[\equiv \frac{g water/cm^3 swollen polymer}{g water/cm^3 solution}\right] \tag{3}$$

The C_W^m value can be related to the volume fraction of water in the polymer membrane (ϕ_W) as follows [4,8]:

$$C_W^m = \phi_W \frac{M_W}{\overline{V}_W} \tag{4}$$

where M_W is the water molecular weight (i.e., 18 g/mol). Eq. (3) can thus be rewritten as:

$$K_W = \frac{\phi_W M_W}{C_W \overline{V}_W} \tag{5}$$

For sufficiently dilute solutions, such as pure water, C_W can be approximated as the density of pure water (ρ_W). The partial molar volume of water in the polymer membrane, $\overline{V}_W$, is assumed to be identical to the molar volume of water in solution (i.e., 18 cm^3/mol); in addition, the contiguous water contacting the polymer membrane is presumed to have the density of pure water (ρ_W). With these reasonable assumptions, Eq. (5) can be rewritten as follows [4,8]:

$$K_W = \phi_W \tag{6}$$

Thus, K_W is equal to the volume fraction of water in the polymer membrane, and this approximation is used to estimate the K_W value based on water uptake measurements.

Pure water flux, J_w, was measured at a constant transmembrane pressure difference in a cross flow filtration system at 25 °C [1,4,7,8,40]. Six cross flow cells were connected in series, and the effective mass transfer area of each cell was 18 cm^2. The feed solution was ultra-pure deionized water (from a Millipore MilliQ system, Darmstadt, Germany), and feed flow rate was 1 gallon/min (3.8 L/min). The applied feed (i.e., upstream) pressure was 400 psig (27.6 bar) and the permeate (i.e., downstream) pressure was atmospheric pressure (1.0 bar). A refrigerated water bath (Neslab RTE 17, Thermo Scientific, Waltham, MA) was used to maintain a constant feed temperature of 25 °C. The steady-state water flux (J_w) can be calculated by recording the volume of permeate (i.e., water) (ΔV) passing through a membrane area (A) as a function of time (Δt):

$$J_w = \frac{\Delta V}{A \bullet \Delta t} \tag{7}$$

Hydraulic water permeability (P_W^H, $L \bullet \mu m/(m^2 \bullet h \bullet bar)$) is defined from the water flux (J_w), membrane thickness (L), and pressure difference (Δp) as follows [4,8,40,41]:

$$P_W^H = \frac{J_w}{\Delta p} \bullet L \tag{8}$$

According to the solution-diffusion model [39,42], the water concentration gradient induced by the pressure difference in the dense membrane leads to water diffusion. If the Flory-Huggins model is employed to consider the influence of water activity on water uptake of the polymer membrane, as previously reported [4,8,41], the diffusive water permeability (P_W^D, cm^2/s) can be expressed in terms of hydraulic water permeability (P_W^H) as follows [4,8,43–45]:

$$P_W^D = D_W \bullet K_W = P_W^H \bullet \frac{RT}{\overline{V_W}}[(1 - K_W)^2(1 - 2\chi K_W)] \tag{9}$$

where D_W is the concentration-averaged, effective water diffusivity of the polymer membrane, R is the ideal gas constant, T is absolute temperature, and χ is the Flory-Huggins interaction parameter. Based on the Flory-Huggins theory, χ can be used to relate the water activity (a_W) in a swollen polymer to the water concentration in the polymer as follows [4,8,41,46,47]:

$$ln a_W = ln K_W + (1 - K_W) + \chi(1 - K_W)^2 \tag{10}$$

Since, for each membrane sample, the water concentration in an equilibrated polymer membrane can be experimentally measured, and because the pure water has an activity value, a_W, of 1, χ values can be estimated. Using this information, P_W^D can be calculated from P_W^H and χ values using Eq. (10).

The concentration-averaged, effective water diffusivity (D_W, cm^2/s) can be calculated from P_W^D and K_W values as [4,8,41]:

$$D_W = \frac{P_W^D}{K_W} \tag{11}$$

2.4.2. Estimation of P_s, K_s, and D_s

The salt solubility (i.e., salt partition coefficient, K_s) is defined as the ratio of the salt (NaCl) concentration in the polymer membrane, to the salt concentration (i.e., 1.0 M) in the contiguous solution as follows:

$$K_s = \frac{C_S^m}{C_S}\left[\equiv \frac{gNaCl/cm^3 swollen membrane}{gNaCl/cm^3 solution}\right] \tag{12}$$

K_s values were measured using desorption experiments at atmospheric pressure and ambient temperature [8,48]. Membrane samples of known dimensions (diameter = 2.2 cm) were soaked in 50 ml of 1.0 M NaCl solution for between 48 and 72 h [48]. The required soaking time was estimated based on L^2/P_s value, where L is the thickness of the film, P_s is the salt permeability of the membrane determined for the particular NaCl solution (i.e., 1.0 M in this study), and the time used was at least 3 times the L^2/P_s value. During this period of time, the membrane samples were expected to absorb an equilibrium amount of ions from the solution. After soaking in the salt solution, the excess salt on the sample surface was removed using tissue paper. The sample was then immersed in a clean tube containing 50 ml of deionized water for at least 3 times the L^2/P_s value, as mentioned above. The samples desorbed the equilibrium amount of ions (chloride ion, Cl^-) to the external deionized water during this period of time, and ion chromatography (ICS-2100, Dionex Corp. Sunnyvale, VA) was used to analyze the concentration of chloride ion in the desorption solution [48]. The amount of NaCl per cm^3 of swollen membrane was calculated using the chloride ion concentration, the volume of desorption solution (50 ml), and sample dimensions.

Salt permeability (P_s) was measured using direct permeation cells with dual chambers (Side-Bi-Side Cells, PermeGear, Hellertown, PA) at atmospheric pressure and ambient temperature. The donor and the receiver chamber glass cells have volumes of 35 ml each, and a polymer membrane coupon was located between two chamber cells. The effective area of mass transfer (A) is 1.77 cm^2. At the start, the donor cell was filled with 1.0 M NaCl solution, and the receiver cell was filled with ultra-pure deionized water. The donor/receiver cells were sealed with Parafilm, and stir bars were used with a magnetic drive in each cell to ensure solution homogeneity. As salt diffuses through the membrane from the donor cell to the receiver cell filled with deionized water, the diffused salt gradually changes the conductivity in the receiver cell. The conductivity in the receiver cell was recorded as a function of time, t, using a conductivity probe (LR325/01, WTW, Oberbayem, Germany) and meter (InoLab Cond 730, WTW, Oberbayem, Germany). The salt concentration in the receiver cell was calculated from the recorded conductivity using the calibration curve, which correlates conductivity to salt concentration. By measuring the salt concentration change over time in the receiver cell, the salt permeability (P_s) can be calculated as follows:

$$-\frac{V_R L}{2A} \ln\left[1 - \frac{2C_R[t]}{C_D[0]}\right] = P_s t \tag{13}$$

where C_R[t] is the salt concentration in the receiver cell at time t, C_D[0] is the initial concentration of salt in the donor cell (i.e., 1.0 M NaCl), V_R is the volume of the donor/receiver cell (i.e., 35 ml), L is the membrane thickness, and A is the membrane area (i.e., 1.77 cm^2).

The salt diffusivity (D_S) can be determined from known P_s and K_s values:

$$D_s = \frac{P_s}{K_s} \tag{14}$$

3. Results and discussion

3.1. Chemical structural characterization of BPS-20K films prepared via different preparation routes

BPS-20K membranes were obtained by utilizing different processing methods (solution casting vs. melt extrusion), PEG composition (molecular weight, $\overline{M_n}$: 200–400 g/mol and concentration 20–30 wt%) during melt extrusion, and PEG extraction temperatures (23 °C, 50 °C and 75 °C) after melt extrusion, as shown in Table 2.

FT-IR was used to characterize the chemical structure of BPS-20K films prepared by different preparation paths. Fig. 2 shows the FT-IR spectra (4000 ~ 600 cm^{-1}) of selected films. The FT-IR spectra of other samples, which are not shown for the sake of brevity, were similar to those in Fig. 2. No significant variations in FT-IR spectra were observed between films prepared via the different preparation routes. ^{1}H NMR was also employed to verify the molecular structure of our BPS-20K films. NMR and FT-IR show no differences in chemical structure between films prepared by the various preparation paths. The ^{1}H NMR spectra of these films are not shown for the sake of brevity, but more information on film formation can be found in our previously published work [32].

Table 2
BPS-20K membranes prepared by different routes.

Processing method	Polymer	PEG $\overline{M_n}$ [g/mol]	PEG wt%	PEG extraction temp [°C]	PEG extraction time
Solution	BPS-20K	–	–	–	–
Solution	BPS-20K	–	–	50[a]	1 h[a]
Solution	BPS-20K	–	–	75[a]	1 h[a]
Extrusion	BPS-20K	200	20	23	4 days
Extrusion	BPS-20K	400	20	23	4 days
Extrusion	BPS-20K	200	30	23	4 days
Extrusion	BPS-20K	200	20	50	1 h
Extrusion	BPS-20K	200	20	75	1 h

[a] Solution cast BPS-20K films do not contain PEG in the samples; however, these samples were soaked in DI water at high temperatures (50 °C, 75 °C) for 1 h for comparison with melt-extruded samples from which PEG was extracted into DI water at high temperatures.

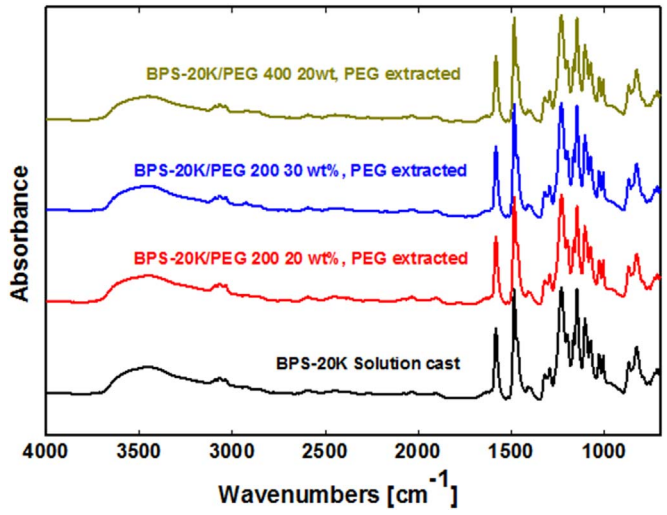

Fig. 2. FT-IR (ATR mode) spectra of BPS-20K films prepared by different preparation paths. FT-IR spectra have been displaced vertically for easier viewing. PEG was extracted from these extruded BPS-20K/PEG films by soaking in DI water at ambient temperatures for four days.

To further determine if there were any chemical changes in BPS-20K due to the different preparation steps, some melt-extruded, PEG-extracted (i.e., "extruded/extracted") films were dissolved in DMAc and solution cast again for further studies. As shown in Table 3 (marked as "Extrusion→Solution"), one extruded/extracted BPS-20K film (BPS-20K/PEG 200 g/mol 20 wt%, PEG extracted at 75 °C for 2 days) was dried and dissolved in DMAc and solution cast on a glass plate, following the drying protocol described previously [8]; the motivation for using this particular extruded/extracted BPS-20K/PEG 200 g/mol sample is that 75 °C is the highest water temperature employed for PEG extraction, and 2 days is the longest soaking time at high temperatures during PEG extraction. In other words, this sample represents the most extreme processing conditions used in this study.

Note that the BPS-20K polymer used for "Extrusion→Solution" experiments in Table 3 has slightly higher molecular weight ($\overline{M}_w$ = 31,300 g/mol) than that of the BPS-20K polymer ($\overline{M}_w$ = 29,700 g/mol) that was used in this study. The BPS-20K of $\overline{M}_w$ = 31,300 g/mol was used because the "Extrusion→Solution" experiments required large amounts of film materials, and BPS-20K of $\overline{M}_w$ = 29,700 g/mol was not sufficient to supply this experiment. However, their molecular weights are in a similar range, and their salt permeability and T_g are also quite similar, as seen in Table 3.

The salt permeability and T_g of this "Extrusion→Solution" sample are in a range similar to those of solution cast, control BPS-20K films, within the uncertainty of our measurements. This result further confirms that the different preparation routes in this study do not change the chemical structure of BPS-20K films.

3.2. Transport properties of BPS-20K films prepared by different routes

Water and salt transport properties of BPS-20K membranes prepared by different routes are summarized in Tables 4, 5, respectively. These melt-extruded, PEG-extracted (i.e., "extruded/extracted") BPS-20K membranes were kept in DI water before testing. Changes in soaking time in DI water (i.e., one hour to 1 week) before testing at ambient temperature did not influence transport properties of these membranes. Similar observations were reported by Xie et al. [8].

Fig. 3 shows water permeability (3a) and water diffusivity (3b) in BPS membranes prepared by different processing methods as a function of water uptake in volume fraction (K_w, [cm^3 H_2O/cm^3 hydrated polymer]). The motivation for plotting the data versus water uptake comes from the work of Yasuda *et al.* and previous studies from our research group suggesting that membrane transport properties are governed by free volume [8,49–52]. In hydrated polymers, free volume is often proportional to sorbed water content (i.e., water uptake). When plotted in this manner, Fig. 3, a strong correlation between water transport properties and water uptake appears as expected. Water permeability and diffusivity increase as water uptake increases. Similar trends can be found with salt transport properties in Fig. 4, as salt solubility, permeability and diffusivity increase as water uptake increases. Therefore, this free volume-based theory can be used to correlate the diffusion of water and salt across the BPS membranes with water uptake [8,51]; further correlation with free volume theory will be discussed in Section 3.3.

Compared to the solution cast BPS-20K membrane, the extruded/extracted BPS-20K membranes prepared using various PEG $\overline{M}_n$ and concentrations and different PEG extraction temperatures (23 °C, 50 °C and 75 °C) exhibit significantly higher water uptake, as shown in Fig. 3a. Even the extruded/extracted BPS membranes prepared using the lowest PEG concentration (20 wt%), the lowest molecular weight (200 g/mol), and the lowest PEG extraction temperature (23 °C) have 60% higher water uptake than solution cast BPS-20K samples. Note that 20 wt% is the minimum PEG concentration required for melt extrusion to produce membranes of uniform thickness in this study [34].

3.2.1. Effect of PEG molecular weight and concentration

BPS-20K films prepared with higher PEG molecular weight and higher concentration during extrusion have higher water uptake and higher permeability after PEG has been extracted from the films. This trend is consistent with previous literature reporting the use of PEGs as pore forming additives in preparation of porous membranes by phase inversion methods [54–58], even though the BPS-20K membranes in this study were prepared by solvent-free melt extrusion, not by phase inversion methods. Previously, Xu and others used PEG molecular weights ranging between 200 g/mol and 10,000 g/mol as additives to fabricate polyethersulfone (PES) hollow-fiber membranes via phase inversion methods; they reported pure water flux increases from 22.0 to 64.0 L m^{-2} h^{-2} bar^{-1} as PEG molecular weight changed from 200 g/mol to 10,000 g/mol [55]. Similar observations can be found elsewhere [54–63].

Qualitatively, PEG extraction from the extruded BPS-20K films

Table 3
Salt permeabilities (P_s) and glass transition temperatures (T_g) of BPS-20K membranes prepared *via* different routes.

Processing method	Polymer	$\overline{M}_w$ [g/mol]	PEG $\overline{M}_n$ [g/mol]	PEG wt%	PEG extraction temp [°C]	PEG extraction time	P_s [10^{-9} cm^2/s]	T_g [°C]
Solution	BPS-20K	29,700	–	–	–	–	0.058 ± 0.007	256
Solution	BPS-20K	31,300	–	–	–	–	0.054 ± 0.002	256
Extrusion	BPS-20K	31,300	200	20	75	2 days	8.565 ± 0.035	256
Extrusion →Solution[a]	BPS-20K	31,300	200	20	75	2 days	0.076 ± 0.020	256

[a] "Extrusion→Solution" indicates that (1) the extruded BPS/PEG film was soaked in DI water at given temperature and time to remove most of PEG from the film, and then (2) dried at 110 °C in a vacuum oven for 24 h to remove residual water from the film, and subsequently (3) dissolved in DMAc (10 wt% polymer solution), and solution cast on a glass plate, following the drying protocol reported previously [8].

Table 4
Water permeabilities, water diffusivities and water uptakes (water solubilities) of BPS-20K films prepared by different routes.

Processing method	Polymer	PEG $\overline{M}_n$ [g/mol]	PEG wt%	PEG extraction temp [°C]	PEG extraction time	χ[a]	P_w^H [L μm/ (m^2 h bar)]	P_w^D [10^{-6} cm^2/s]	D_w [10^{-6} cm^2/s]	K_w
Solution	BPS-20K	–	–	–	–	1.73	0.030 ± 0.003	0.115	1.15	0.10 ± 0.03
Solution	BPS-20K	–	–	50	1 h	1.50	0.049 ± 0.009	0.187	1.37	0.14 ± 0.01
Solution	BPS-20K	–	–	75	1 h	1.45	0.093 ± 0.007	0.355	2.28	0.15 ± 0.00
Extrusion	BPS-20K	200	20	23	4 days	1.41	0.263 ± 0.047	1.00	6.59	0.16 ± 0.02
Extrusion	BPS-20K	400	20	23	4 days	1.30	0.301 ± 0.015	1.15	6.20	0.19 ± 0.01
Extrusion	BPS-20K	200	30	23	4 days	1.09	1.73 ± 0.18	6.61	24.30	0.27 ± 0.01
Extrusion	BPS-20K	200	20	50	1 h	1.30	0.528 ± 0.020	2.02	1.37	0.19 ± 0.01
Extrusion	BPS-20K	200	20	75	1 h	1.18	1.135 ± 0.065	4.33	2.28	0.23 ± 0.02

[a] χ was calculated using Eq. (10).

Table 5
Salt permeabilities, salt diffusivities and salt solubilities in BPS-20K films prepared by different routes.

Processing method	Polymer	PEG $\overline{M}_n$ [g/mol]	PEG wt%	PEG extraction temp [°C]	PEG extraction time	P_s [10^{-9} cm^2/s]	D_s[a] [10^{-7} cm^2/s]	K_s
Solution	BPS-20K	–	–	–	–	0.058 ± 0.007	0.029 ± 0.006	0.020 ± 0.004
Solution	BPS-20K	–	–	50	1 h	0.12 ± 0.01	0.068 ± 0.004	0.018 ± 0.001
Solution	BPS-20K	–	–	75	1 h	0.42 ± 0.01	0.14 ± 0.02	0.031 ± 0.004
Extrusion	BPS-20K	200	20	23	4 days	2.47 ± 0.25	0.308 ± 0.029	0.08 ± 0.007
Extrusion	BPS-20K	400	20	23	4 days	4.03 ± 0.15	0.598 ± 0.071	0.068 ± 0.008
Extrusion	BPS-20K	200	30	23	4 days	55.40 ± 1.78	4.78 ± 0.21	0.116 ± 0.005
Extrusion	BPS-20K	200	20	50	1 h	10.3 ± 0.84	1.16 ± 0.12	0.089 ± 0.010
Extrusion	BPS-20K	200	20	75	1 h	26.0 ± 3.1	2.32 ± 0.04	0.112 ± 0.002

[a] Relative variance of D_s was calculated by error analysis [53].

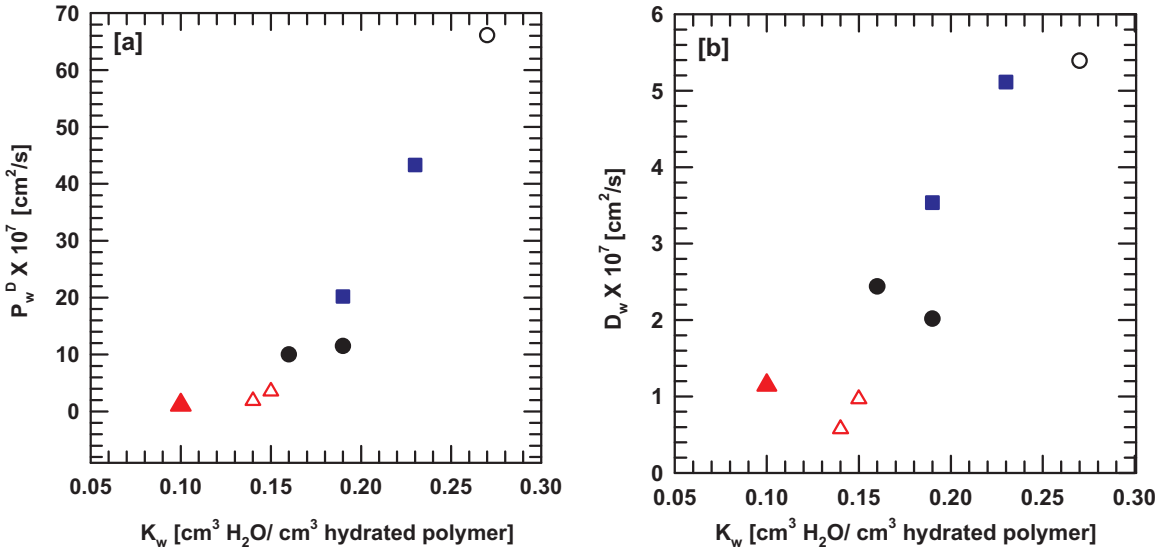

Fig. 3. [a] Diffusive water permeability (P_w^D), and [b] water diffusivity (D_w) as a function of water uptake in volume fraction (K_w, [cm^3 H_2O /cm^3 hydrated polymer]). Symbols are (from left to right): 1) solution cast, control BPS-20K film (▲); 2, 3) solution cast BPS-20K film, soaked in 50 °C (left △) and 75 °C (right △) for 1; h 4, 5) extruded/extracted BPS-20K/PEG ($\overline{M}_n$: 200 (left •), 400 g/mol (right •)) 20 wt% films, soaked in 23 °C for 4 days; 6, 7) extruded/extracted BPS-20K/PEG 200 g/mol 20 wt%, soaked in 50 °C (left ■) and for 75 °C (right ■) for 1h; 8) extruded/extracted BPS-20K/PEG 200 g/mol 30 wt%, soaked in 23 °C for 4 days (○).

could generate additional free volume, and as PEG molecular weight and PEG concentration in BPS-20K/PEG films increase, the free volume could also increase, as reflected in increased water uptake. A complete study to probe the free volume element of these samples has not been done but will be the subject of future investigations.

At a fixed PEG concentration of 20 wt%, as PEG molecular weight increased from 200 g/mol to 400 g/mol, water uptake increased by almost 20%. At a fixed PEG molecular weight of 200 g/mol, as PEG concentration increased from 20 wt% to 30 wt%, water uptake increased 1.7 times. The water uptake increase induced by raising PEG concentration from 20 wt% to 30 wt% is greater than that achieved by increasing PEG molecular weight from 200 g/mol to 400 g/mol. Overall, as water uptake increases, water permeability (Fig. 3a) and water diffusivity (Fig. 3b) also increase, consistent with the findings of Yasuda et al.

3.2.2. Effect of PEG extraction temperature

The rate of PEG extraction from extruded BPS/PEG membranes is affected by temperature [34]. PEG extraction kinetics are faster at higher temperatures and, therefore, only one hour of soaking time was required in water at high temperatures (i.e., 50 °C and 75 °C) to remove most of the PEG from BPS-20K/PEG films [33,34]. More details about the PEG extraction kinetics have appeared previously [33].

As shown in Table 2, starting from one BPS-20K membrane

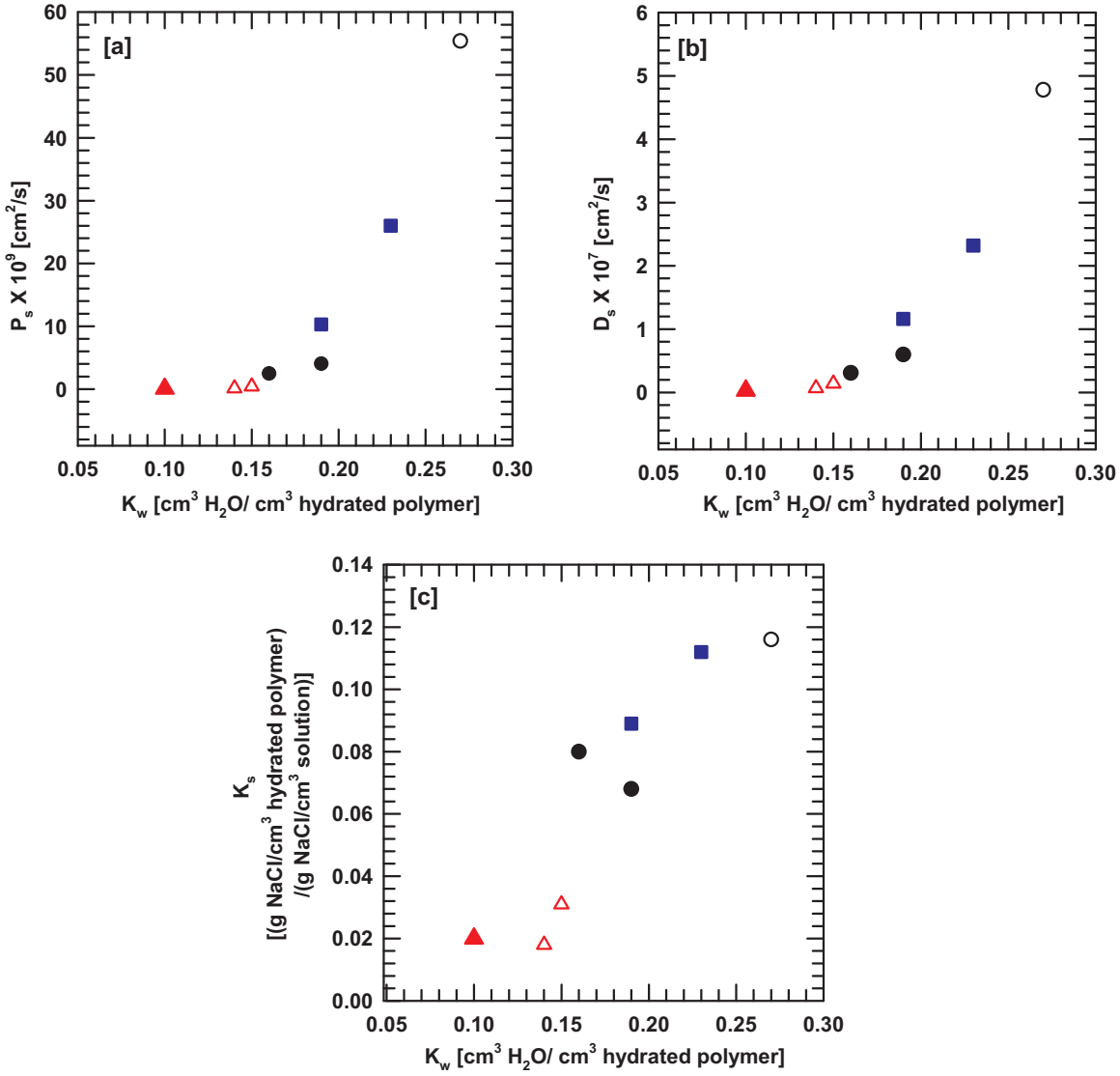

Fig. 4. [a] salt permeability (P_s), [b] salt diffusivity (D_s), and [c] salt solubility (K_s [(g NaCl/cm^3 hydrated polymer/(g NaCl /cm^3 solution)]) as a function of water uptake in volume fraction (K_w, [cm^3 H_2O /cm^3 hydrated polymer]). Symbols used are identical to those described in the caption from Fig. 3, except as otherwise noted.

prepared with the same PEG molecular weight (200 g/mol) and PEG concentration (20 wt%) (i.e., BPS-20K/PEG 200 g/mol 20 wt%), PEG was removed from the BPS/PEG films by soaking the films at different temperatures (23 °C, 50 °C and 75 °C). Soaking time, which varied at different temperatures, was chosen based on the minimum required time to remove most of the PEG from the BPS-20K/PEG films. The amount of PEG remaining in the sample after soaking is below the detection limit of ^{1}H NMR analysis [17,33].

Consistent with previous literature reports [4,35–37], immersing the extruded BPS-20K films in DI water at 75 °C increased the water uptake by 40% over that of the same films soaked in DI water at ambient temperature. Thermal treatment had a similar influence on the water uptake of our solution cast BPS-20K films. After thermal treatment, these films exhibited roughly 50% higher water uptake than that of solution-cast control films. Further soaking at ambient temperature (23 °C) does not alter the transport properties of BPS-20K films, whereas prolonged soaking of samples at high temperatures can significantly influence the transport properties. Similarly, Xie *et al.* observed that soaking solution cast BPS-32 membranes (K and H form) at 50 °C, 75 °C and in boiling water changed the transport properties substantially. A BPS-32K film soaked in boiling water for four hours showed a 2.3-fold water permeability increase, while salt permeability increased by a factor of 8 and water uptake by a factor of 1.5. They propose that these properties are sensitive to thermal processing steps because the glassy BPS polymers would be in a non-equilibrium state below their T_g [4]. Similar observations have been reported with perfluorinated sulfonated polymer membranes (Nafion®) [35–37].

In summary, extruded/extracted BPS-20K films show higher water uptake than that of solution cast BPS-20K membranes, and as PEG molecular weight and concentration used during extrusion increases and as PEG extraction temperature increases, water uptake increases. Consistent with the findings of Yasuda *et al.* regarding NaCl transport through hydrated polymers [49], as water uptake increases, water and salt permeabilities and diffusivities also increase, as shown in Figs. 3 and 4.

3.3. Correlation with free volume theory

In this study, starting from one polymer, BPS-20K, different preparation routes led to different transport properties. The changes in preparation routes significantly influence water uptake and water and salt permeabilities, and it was of interest to probe whether the water uptake and water and salt transport properties could be further correlated using free volume theory.

From free volume theory, diffusivity (D) can be written in terms of free volume of the polymer (v_f) as [49]:

$$D \propto \exp[-(\frac{v^*}{v_f})] \tag{15}$$

where v^* is the characteristic volume needed for the diffusion of a small penetrant molecule through a polymer. If the free volume of a membrane scales linearly with the volume fraction of diluent in the polymer, then diffusivity scales *exponentially* with changes in the volume fraction of diluent in the polymer. In hydrated polymers such as those in our study, the volume fraction of water in the hydrated polymer is expressed as water uptake, K_w.

Yasuda *et al.* proposed, based on free volume theory, that the free volume of a hydrated polymer could be written as the summation of the free volume of the polymer and the free volume of water as [49]:

$$v_f = K_w \bullet v_{f,H_2O} + (1 - K_w) \bullet v_{f,polymer} \tag{16}$$

where v_{f,H_2O} is the free volume of water and $v_{f,polymer}$ is the free volume of dry polymer. Because the permeation of salt (NaCl) across a pure (dehydrated) polymer is likely to be negligible, most salt probably permeates through the hydrated regions of polymers; thus, the available free volume for salt permeation is the free volume added by water, and Eq. (17) becomes [49]:

$$v_f \cong K_w \bullet v_{f,H_2O} \tag{17}$$

Therefore, the salt diffusivity (D_s) in hydrated polymers can be expressed as [49]:

$$\log D_s = \log D_0 - B(\frac{1}{K_w} - 1) \tag{18}$$

where D_0 is the salt (NaCl) diffusivity in pure water at 25 °C (i.e., 1.47×10^{-5} cm^2/s [8]), and B is a proportionality constant in terms of v^* and v_{f,H_2O}. Therefore, when salt diffusivity is plotted as a function of $1/K_w$, a linear relationship is expected, starting at $1/K_w = 1$, the salt diffusivity in pure water.

Fig. 5 shows the water and salt diffusivity from this study plotted as a function of $1/K_w$, along with data from previous studies for comparison [8]. The dashed lines through the data are the fits to Yasuda's model. Both water and salt diffusivity scale exponentially with $1/K_w$, indicating that a reasonable empirical analysis can be done using Yasuda's model. Furthermore, the slope of the salt diffusivity versus $1/K_w$ is steeper than that of water diffusivity versus $1/K_w$, consistent with previous reports [8]. Since hydrated Na^+ and Cl^- ions are larger than a water molecule, larger penetrants exhibit a stronger dependence on free volume than do smaller molecules. For instance, when water uptake increased 2.3 times in this study (from the lowest to the highest value), the water diffusivity increased 14 times, but the salt diffusivity increased 165 times.

Additionally, other BPS polymers, i.e., solution cast BPS-K and BPS-H, from previous studies are shown for comparison [8]. The motivation for this comparison was to check whether the differences in water and salt transport properties of the extruded/extracted BPS-20K films in this study could be brought about by varying the sulfonation level and ionic forms in the BPS polymers at fixed processing history. Overall, the change in water and salt diffusivity in the extruded/extracted BPS-20K films in this study were indeed brought about by changing the sulfonation level (sulfonation levels between 20 and 40 mol%) and ionic forms (K and H forms) in solution cast BPS polymers. This observation implies that, like other glassy polymers, BPS polymers are sensitive to processing history. Similar trends can be found with water and salt permeabilities, and these will be discussed further in this section.

In particular, the salt diffusivity of extruded/extracted BPS-20K films in this study showed a similar fit to Yasuda's model as that of the salt diffusivity in the solution cast BPS polymers. The water diffusivity of the extruded/extracted BPS-20K films was somewhat higher, with a slope of water diffusivity versus $1/K_w$ similar to that of solution cast BPS polymers.

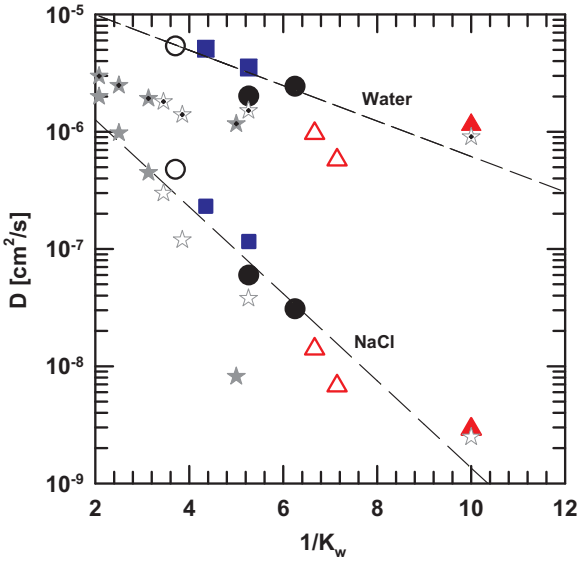

Fig. 5. Water and salt diffusivity (D_w and D_s) versus $1/K_w$ of BPS-20K membranes prepared by different routes. Dashed lines are the fit of Yasuda's model to the data. Symbols used in this study (from right to left): 1) solution cast, control BPS-20K film (▲); 2, 3) solution cast BPS-20K film, soaked in 50 °C (right △) and 75 °C (left △) for 1 h; 4, 5) extruded/extracted BPS-20K/PEG ($\overline{M}_n$: 200 (right •), 400 g/mol (left •)) 20 wt% films, soaked in 23 °C for 4 days; 6, 7) extruded/extracted BPS-20K/PEG 200 g/mol 20 wt%, soaked in 50 °C (right ■) and for 75 °C (left ■) for 1 h; 8) extruded/extracted BPS-20K/PEG 200 g/mol 30 wt%, soaked in 23 °C for 4 days (○). The upper dashed line is a trend line of water diffusivity, whereas the lower dashed line is a trend line of salt diffusivity in this study. Comparison with the solution cast BPS-K and BPS-H films: sulfonation level is 40, 35, 30 and 20 mol%, from left to right [8]. BPS symbols (☆, ★) close to the lower dashed line (a trend line of salt diffusivity in this study) are salt diffusivities of BPS-K (☆) and BPS-H (★) films, while BPS symbols (☆, ★) located between the upper dashed line (a trend line of water diffusivity in this study) and the lower dashed line are the water diffusivities of BPS-K (☆) and BPS-H (★) films.

Fig. 6 shows the salt solubility (K_s) versus water solubility (K_w) of BPS-20K films in this study, along with the data from previous studies for comparison [8,49]. The salt solubility (i.e., salt partition coefficient K_s) is defined as the ratio of the salt concentration in the polymer membrane to the salt concentration in the contiguous solution (see Eq. (12)). Yasuda *et al.* suggested a simplest approximation that, in hydrated polymers, the amount of salt sorbed in the polymer (K_s) will likely increase with an increase in sorbed water (K_w). For example, some polymers, such as hydroxypropylmethacrylate-glycerol methacrylate copolymers (HPMA-GMA), and hydroxylethyl methacrylate (HEMA), etc. from Yasuda's work [49], exhibit salt solubility almost identical to water solubility (i.e., $K_s = K_w$, blue dashed line in Fig. 6) [49].

However, this is not the case for all hydrated polymers. The above simple approximation does not consider other multiple factors governing the salt and water sorption, such as the interactions between salt ions, water, ionic groups in the polymer, and polymer backbone [8,49,64]. For instance, other polymers, such as cellulose acetate (CA), and hydroxylethyl methacrylate-methyl methacrylate copolymers (HEMA-MMA), show lower salt solubility compared to water solubility [8,49]. Similarly, the solution cast BPS-K and BPS-H polymers (sulfonation level of 20–40 mol%) from previous work exhibit significantly lower salt solubility values than water solubility values [7,8]. A lower salt than water solubility indicates that a polymer may prevent salt from being sorbed in the polymer matrix due to interactions between ions, water, and the moieties in the polymer. In particular, BPS polymers have fixed charged groups (i.e., ionic sulfonate groups) that are bound to the polymer backbone, and these fixed charged groups tend to reject the sorption of ions of the same charge, and, therefore, reject salts (i.e., Donnan exclusion effect) [7,8,64].

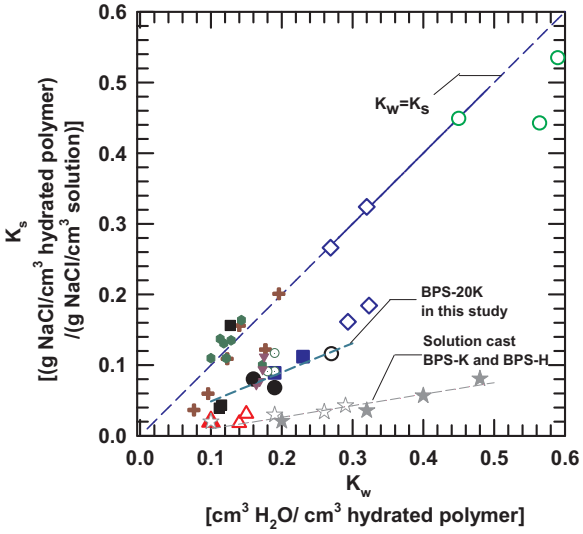

Fig. 6. Salt solubility (K_s, [(g NaCl/cm^3 hydrated polymer/(g NaCl /cm^3 solution)]) as a function of water solubility (K_w, [cm^3 H_2O /cm^3 hydrated polymer]). Blue dashed line in the center represents a line where $K_w = K_s$. Symbols from this study (from left to right): 1) solution cast, control BPS-20K film (▲); 2, 3) solution cast BPS-20K film, soaked in 50 °C (left △) and 75 °C (right △) for 1 h; 4, 5) extruded/extracted BPS-20K/PEG ($\overline{M}_n$: 200 (left •), 400 g/mol (right •)) 20 wt% films, soaked in 23 °C for 4 days; 6, 7) extruded/extracted BPS-20K/PEG 200 g/mol 20 wt%, soaked in 50 °C (left ■) and for 75 °C (right ■) for 1 h; 8) extruded/extracted BPS-20K/PEG 200 g/mol 30 wt%, soaked in 23 °C for 4 days (○). Symbols from literature: Cellulose acetate (CA, ■) [49], hydroxypropyl methacrylate-glycidyl methacrylate copolymers (HPMA-GDMA, ▼) [49], hydroxypropylmethacrylate-glycerol methacrylate copolymers (HPMA-GMA, ◯) [49], hydroxylethyl methacrylate (HEMA, ◇) [49], methyl methacrylate-glycerol methacrylate copolymers (MMA-GMA, ✚) [51], hydroxylethyl methacrylate-methyl methacrylate copolymers (HEMA-MMA, ⊙) [49], cellulose acetate (CA, ✖) [49], and hydroxypropyl methacrylate-methyl methacrylate copolymers (HPMA-MMA, ⬢) [49]. Solution cast BPS-K films (☆) and BPS-H films (★) (sulfonation level is 20, 30, 35 and 40 mol%, from left to right) [8].

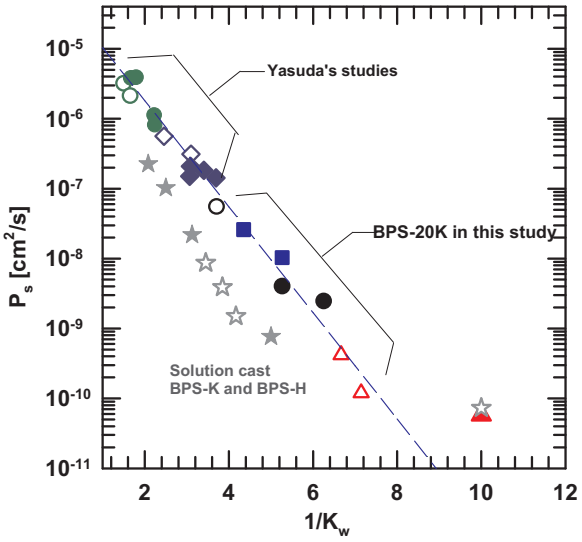

Fig. 7. Salt permeability (P_s) versus $1/K_w$. Symbols from this study: description of symbols are identical to the caption from Fig. 5, except as otherwise noted. Blue dashed line is the fitting line of data from Yasuda's work from Ref. [49]. Symbols from literature: BPS-K films (☆) and BPS-H films (★) (sulfonation level is 40, 35, 30 and 20 mol%, from left to right) [8]. Hydroxypropylmethacrylate-glycerol methacrylate copolymers (HPMA-GMA, ◯: determined from direct permeation, ●: calculated from $P_s = D_s \bullet K_s$) [49], hydroxylethyl methacrylate (HEMA2, ◇: determined from direct permeation, ◆: calculated from $P_s = D_s \bullet K_s$) [8,49].

Here, our extruded/extracted BPS-20K films exhibit somewhat higher salt solubility values than that of the solution cast BPS-20K film, and the salt solubility values are located far lower than the blue dashed line ($K_s = K_w$) in Fig. 6. The increased salt solubility in the extruded/extracted BPS-20K films is likely due to the increased water uptake, consistent with free volume theory. As the water uptake increased at a fixed sulfonation level (i.e., 20 mol%), the fixed charge concentration in the samples could be lowered somewhat by that increased water uptake; thus, the Donnan exclusion effect could diminish, resulting in higher salt solubility. Still, the salt solubility values of these samples are lower than water solubility values (i.e., $K_s < K_w$), since the Donnan exclusion effect resulting from the ionic sulfonate groups persists.

On the other hand, our extruded/extracted BPS-20K films show rather higher salt solubility values than do those of solution cast BPS films at similar water solubility values. Because the chemical structures of the BPS polymers used for this comparison are different in terms of sulfonation level and ionic forms from those of the BPS-20K films in this study, direct comparison is difficult. However, with a rough comparison, our extruded/extracted BPS-20K films do show somewhat higher salt solubility values than those of solution cast BPS-30K, BPS-35K, and BPS-40K films at similar water solubility values. This is likely due to the lower fixed charge concentration (i.e., sulfonation level = 20 mol%) in our BPS-20K films compared to the fixed charge concentration (i.e., sulfonation level = 30, 35, 40 mol%) in these solution cast BPS-K films. As the fixed charge concentration decreases, the Donnan exclusion effect also decreases [64].

Fig. 7 shows salt permeability (P_s) as a function of $1/K_w$ of BPS-20K films found in this study and, for comparison, from polymers in previous studies [7,8,49]. In Yasuda's work with highly hydrated polymers such as hydroxypropylmethacrylate-glycerol methacrylate copolymers (HPMA-GMA) and hydroxylethyl methacrylate (HEMA), salt permeability increases as $1/K_w$ decreases, as indicated by the blue dashed line [8,49]. For the highly hydrated, uncharged hydrogels from Yasuda's work, the major contribution of added free volume (i.e., sorbed water uptake, K_w) to salt permeability arises from its effect on salt diffusivity, as salt diffusivity scales exponentially with $1/K_w$.

Similar to these highly hydrated polymers, the extruded/extracted BPS-20K films in this study follow the trend of Yasuda's studies, as shown in Fig. 7: for the extruded/extracted BPS-20K films, the main contribution of increased free volume, as indicated by the increased water uptake, to salt permeability is likely to its influence on salt diffusivity. The reason that the extruded/extracted BPS-20K membranes follow a trend similar to that of highly hydrated, uncharged hydrogels from Yasuda's work could be due to their somewhat higher salt solubility compared to that of solution cast BPS polymers at similar water solubility values (see Fig. 6).

On the other hand, data from solution cast BPS-H and BPS-K polymers from previous studies fall below the trend line of Yasuda's work and also do not show a simple linear relationship between salt permeability and $1/K_w$. Xie et al. suggested that this difference is due to the significantly lower salt solubility of these polymers relative to the highly hydrated polymers in Yasuda's studies [8] (see Fig. 6).

3.4. The water/salt selectivity of melt processed BPS-20K films

In order to characterize the polymer membranes' intrinsic ability to separate water and salt for desalination applications, the water/salt permeability selectivity ($\alpha_{W/S}$) is defined as the ratio of diffusive water permeability (P_W^D) to salt permeability (P_S) as follows [39,41–43,65]:

$$\alpha_{W/S} = \frac{P_W^D}{P_S} = \frac{D_W}{D_S} \bullet \frac{K_W}{K_S} \tag{19}$$

where D_W/D_S is the water/salt diffusivity selectivity, and K_W/K_S is the water/salt solubility selectivity. Based on the solution-diffusion model, both the water/salt diffusivity selectivity (D_W/D_S) and solubility selectivity (K_W/K_S) contribute to the water/salt permeability selectivity of a polymer membrane. With this perspective, the water/salt diffusivity selectivity (Fig. 8), solubility selectivity (Fig. 9), and permeability selectivity (Fig. 10) are plotted to show the water and salt separation

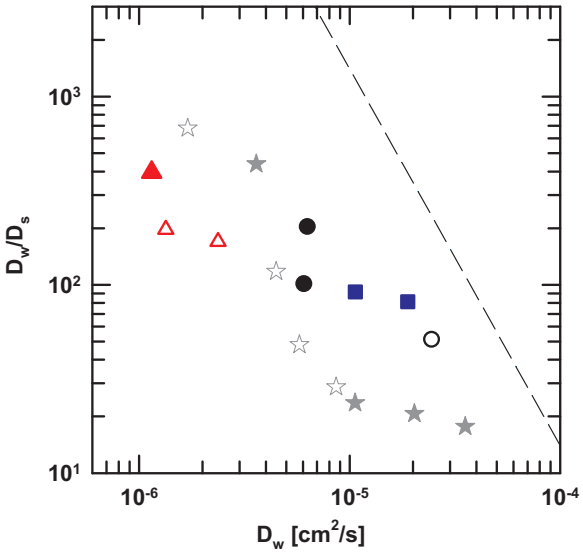

Fig. 8. Water/salt diffusivity selectivity (D_W/D_S) as a function of water diffusivity (D_W). D_W values were determined by using Eqs. (9) and (10), assuming $(1-K_W)^2(1-2\chi K_W) = 1$. The dashed line represents the upper bound from Ref. [64]. Description of symbols are identical to the caption from Fig. 3, except as otherwise noted.

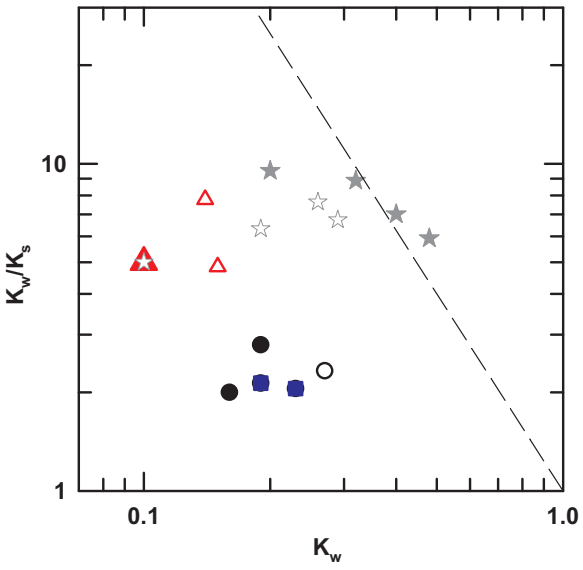

Fig. 9. Water/salt solubility selectivity (K_W/K_S) as a function of water solubility (K_W). The dashed line represents the upper bound from Ref. [64]. Description of symbols are identical to the caption from Fig. 3, except as otherwise noted.

performance of the extruded/extracted BPS-20K films in this study.

Fig. 8 shows the water/salt diffusivity selectivity (D_W/D_S) as a function of water diffusivity (D_W) of the BPS-20K membranes used in this study and a series of solution cast BPS polymers studied previously for comparison [8]. The dashed line is the so-called upper bound of diffusion selectivity versus water diffusivity, representing the best performance of currently available materials [4,8,39,64], and will be discussed further later in this section. Overall, for the extruded/extracted BPS-20K films in this study, as PEG molecular weight and concentration used during extrusion increases, and as PEG extraction temperatures increase, the extruded/extracted BPS-20K films exhibit higher water diffusivity and lower water/salt diffusivity selectivity toward the upper bound, and a general trade-off relationship can be found between these two variables. Also, the previous solution cast BPS polymers follow an overall trade-off relationship between water/salt diffusivity selectivity and water diffusivity; i.e., the BPS polymers with

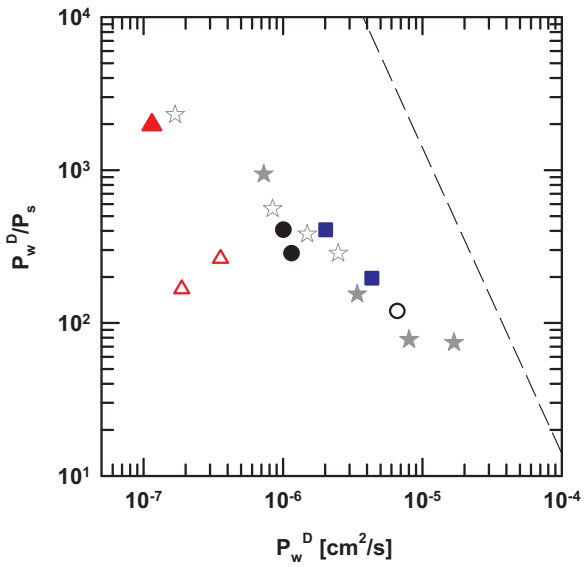

Fig. 10. Water/salt permeability selectivity (P_w^D/P_S) as a function of diffusive water permeability (P_w^D). The dashed line represents the upper bound from Ref. [64]. For proper comparison, P_w^D were determined using Eq. (9), assuming $(1-K_W)^2(1-2\chi K_W) = 1$. Description of symbols are identical to the caption from Fig. 3, except as otherwise noted.

higher sulfonation levels and in acid (H) form showed lower water/salt diffusivity selectivity and higher water diffusivity.

Fig. 9 shows the water/salt solubility selectivity (K_W/K_S) as a function of water solubility (K_W) of both the BPS-20K membranes used in this study and previously studied BPS polymers. In general, the extruded/extracted BPS-20K films using higher PEG molecular weight and concentration during extrusion and higher PEG extraction temperatures show higher water solubility and lower water/salt solubility selectivity; in addition, an overall trade-off relationship is found. The water/salt solubility selectivity of extruded/extracted BPS-20K films is somewhat lower than that of solution cast BPS-20K polymer due to the increased salt solubility in these films. Figs. 8 and 9 show that the water/salt diffusivity selectivity is larger than the solubility selectivity of the extruded/extracted BPS-20K films, similar to that of solution cast BPS polymers in literature [8].

Lastly, Fig. 10 shows the water/salt permeability selectivity (P_w^D/P_S) versus diffusive water permeability (P_w^D) of BPS-20K membranes used in this study and solution cast BPS polymers studied previously [8]. According to the permeability-selectivity trade-off relationship, which is often used to correlate permeability and selectivity for gas separation membranes, a polymer membrane that has higher permeability has a tendency to sacrifice selectivity [8,39,64]. The dashed line is the so-called upper bound of permeability selectivity versus water permeability, representing the best performance of currently available materials [4,39,64].

For the extruded/extracted BPS-20K films, as water permeability increased, permeability selectivity decreased parallel to the upper bound, in a trend similar to that of other solution cast BPS polymers. That is, as the sulfonation level increased and the ionic form is acid (H) form, water permeability increased and permeability selectivity decreased [7,8,10]. However, the extruded/extracted BPS-20K films show higher permeability and lower selectivity than those of solution cast BPS-20K films. As PEG molecular weight and concentration increases and as PEG extraction temperature increases, permeability also increases and selectivity decreases.

The differences in selectivity-permeability of the extruded/extracted BPS-20K films in this study can be achieved by varying the sulfonation level between 20 mol% and 40 mol% and ionic forms (K and H forms) in the BPS polymers at fixed processing history.

Interestingly, the extruded/extracted BPS-20K/PEG 20 wt% films exhibit permeability selectivity similar to that of solution cast BPS-30K and BPS-35K polymers, whereas the extruded/extracted BPS-20K PEG 200 g/mol 30 wt% films fall into a permeability selectivity range similar to that of solution cast BPS-35H polymer. This implies that BPS polymers are sensitive to processing history, similar to other glassy polymers; as a result, in addition to varying the chemical structure of the polymer, varying the processing method also provides extra freedom to modify polymer transport properties.

The fundamental basis for this difference between the samples prepared by different processing routes may arise from the changes in free volume elements between samples prepared via different routes, and a complete study to probe the free volume elements of these samples will be the subject of future investigation.

4. Conclusions

The effect of different membrane processing routes on the water and salt transport properties of glassy, sulfonated polysulfone (BPS) polymers was explored in this study. BPS-20K membranes were prepared by melt processing using poly(ethyelene glycol) (PEG) $\overline{M}_n$ (200 ~ 400 g/mol) as plasticizers at concentrations of 20 wt% to 30 wt%, and at various PEG extraction temperatures. Water and salt transport properties of BPS-20K membranes prepared via different processing routes correlated well with water uptake, consistent with free volume theory. The extruded/extracted BPS-20K films have higher water uptake values than do those of solution cast membranes. As PEG molecular weight and concentration used during extrusion increases, and as PEG extraction temperature increases, water uptake also increases. With increased water uptake, water and salt permeabilities and diffusivities increase, consistent with Yasuda *et al.*'s findings. Compared to the increase in water and salt transport properties as PEG molecular weight increases from 200 g/mol to 400 g/mol, larger water and salt transport property increases are induced by increasing PEG concentration (from 20 wt% to 30 wt%). By immersing the same films at high temperature (75 °C), water uptake goes up by 40%.

In general, BPS-20K membranes prepared by different processing routes followed the trade-off relationship between water permeability and water/salt permeability selectivity. The differences in water/salt selectivity-permeability of the extruded/extracted BPS-20K films in this study can be achieved by varying the sulfonation level between 20 mol % and 40 mol% and the ionic forms (K or H forms) in the solution cast BPS polymers at fixed processing history. This implies that BPS polymers are sensitive to processing history, similar to other glassy polymers; as a result, in addition to varying the chemical structure of the polymer, varying the processing method also provides extra freedom to modify polymer transport properties.

Acknowledgements

This work was supported by NSF Science and Technology Center for Layered Polymeric Systems (Grant 0423914). We thank Benny Freeman for his help and guidance. We appreciate Sue Mecham at Virginia Polytechnic Institute and State University for SEC analysis. NSF-MRI (grant 1126534) at Virginia Polytechnic Institute and State University supports SEC analysis equipment. We also appreciate Cara Doherty at CSIRO for discussion. We also appreciate help from Ben Shoulders in the Department of Chemistry at the University of Texas at Austin, who provided valuable advice about analyzing our ^{1}H NMR data.

References

[1] W. Xie, G.M. Geise, B.D. Freeman, H.-S. Lee, G. Byun, J.E. McGrath, Polyamide interfacial composite membranes prepared from m-phenylene diamine, trimesoyl chloride and a new disulfonated diamine, J. Membr. Sci. 403–404 (1–2) (2012) 152–161.

[2] R.J. Petersen, Composite reverse osmosis and nanofiltration membranes, J. Membr. Sci. 83 (1) (1993) 81–150.

[3] C. Linder, O. Kedem, History of nanofiltration membranes 1960 to 1990, in: A.I. Schafer, A.G. Fane, T.D. Waite (Eds.), Nanofiltration: Principles and Applications, Elsevier, New York, 2003.

[4] W. Xie, G.M. Geise, B.D. Freeman, C.H. Lee, J.E. McGrath, Influence of processing history on water and salt transport properties of disulfonated polysulfone random copolymers, Polymer 53 (7) (2012) 1581–1592.

[5] M.Y. Kariduraganavar, R.K. Nagarale, A.A. Kittur, S.S. Kulkarni, Ion-exchange membranes: preparative methods for electrodialysis and fuel cell applications, Desalination 197 (225–246) (2006).

[6] M. Heinzer, M. Lee, R. Van Houten, O. Lane, J.E. McGrath, D.G. Baird, Effects of solvent-casting conditions on the morphology and properties of highly fluorinated poly(arylene ethersulfone) copolymer films for polymer electrolyte membranes, in: Proceedings of Annual Technical Conference - Society of Plastics Engineers, vol. 67, 2009, pp. 606–610.

[7] W. Xie, J. Cook, H.B. Park, B.D. Freeman, C.H. Lee, J.E. McGrath, Advances in membrane materials: desalination membranes based on directly copolymerized disulfonated poly(arylene ether sulfone) random copolymers, Water Sci. Technology : a J. Int. Assoc. Water Pollut. Res. 61 (3) (2010) 619–624.

[8] W. Xie, J. Cook, H.B. Park, B.D. Freeman, C.H. Lee, J.E. McGrath, Fundamental salt and water transport properties in directly copolymerized disulfonated poly(arylene ether sulfone) random copolymer, Polymer 52 (9) (2011) 2244–2254.

[9] F. Wang, M. Hickner, Y.S. Kim, T.A. Zawodzinski, J.E. McGrath, Direct polymerization of sulfonated poly(arylene ether sulfone) random(statistical) copolymer: candidates for next proton exchange membranes, J. Membr. Sci. 197 (1–2) (2002) 231–242.

[10] H.B. Park, B.D. Freeman, Z.-B. Zhang, M. Sankir, J.E. McGrath, Highly chlorine-tolerant polymers for desalination, Angew. Chem. Int. Ed. 47 (32) (2008) 6019–6024.

[11] C. Yu, J.R. Rowlett, C.H. Lee, O.R. Lane, D. Van Houten, M. Zhang, R.B. Moore, J.E. McGrath, Synthesis and characterization of multiblock partially fluorinated hydrophobic poly(arylene ether sulfone)-hydrophilic disulfonated poly(arylene ether sulfone) copolymers for proton exchange membranes, J. Polym. Sci., Part A: Polym. Chem. 51 (10) (2013) 2301–2310.

[12] A. Roy, M.A. Hickner, H.-S. Lee, A. Badami, X. Yu, Y. Li, T. Glass, J.E. McGrath, Transport properties of proton exchange membranes, ECS Trans. 20 (24) (2006) 45–54.

[13] Y. Li, F. Wang, J. Yang, D. Liu, A. Roy, S. Case, J. Lesko, J.E. McGrath, Synthesis and characterization of controlled molecular weight disulfonated poly(arylene ether sulfone) copolymers and their applications to proton exchange membranes, Polymer 47 (11) (2006) 4210–4217.

[14] Y.S. Kim, L. Dong, M.A. Hickner, B.S. Pivovar, J.E. McGrath, Processing induced morphological development in hydrated sulfonated poly(arylene ether sulfone) copolymer membranes, Polymer 44 (19) (2003) 5729–5736.

[15] J. Huang, D.G. Baird, J.E. McGrath, Continuous solution casting and properties of sulfonated poly(arylene ether sulfone) copolymer membranes for fuel cells, in: Proceedings of Annual Technical Conference – Society of Plastics Engineers, vol. 66, 2008, pp. 69–73.

[16] H.J. Oh, B.D. Freeman, J.E. McGrath, C.J. Ellison, S. Mecham, K.-S. Lee, D.R. Paul, Rheological studies of disulfonated poly(arylene ether sulfone) plasticized with poly (ethylene glycol) for membrane formation, Polymer 55 (6) (2014) 1574–1582.

[17] H.J. Oh, B.D. Freeman, J.E. McGrath, C.H. Lee, D.R. Paul, "Thermal analysis of disulfonated poly(arylene ether sulfone) plasticized with poly(ethylene glycol) for membrane formation, Polymer 55 (1) (2014) 235–247.

[18] C.H. Lee, D. VanHouten, O. Lane, J.E. McGrath, J. Hou, L.A. Madsen, J. Spano, S. Wi, J. Cook, W. Xie, H.J. Oh, G.M. Geise, B.D. Freeman, Disulfonated poly(arylene ether sulfone) random copolymer blends tuned for rapid water permeation via cation complexation with poly(ethylene glycol) oligomers, Chem. Mater. 23 (4) (2011) 1039–1049.

[19] P. Bebin, H. Galiano, Processing of sulfonated polysulfone for PEMFC membrane applications: part 2. polymer in salt form, Adv. Polym. Technol. 25 (2) (2006) 127–133.

[20] P. Bebin, H. Galiano, Processing of PEMFC membranes by extrusion: part 1. sulfonated polysulfone in acid form, Adv. Polym. Technol. 25 (2) (2006) 121–126.

[21] J.-.Y. Sanchez, C. Iojoiu, Y. Piffard, N.E. Kissi, F. Chabert, Extrusion of a thermoplastic polymer bearing acid ionic groupings, United States Patent No. 7956095 B2, 2011.

[22] J.-.Y. Sanchez, C. Iojoiu, R. Mercier, M. Marechal, N.E. Kissi, H. Galiano, F. Chabert, Membrane preparation method comprising the extrusion of a thermoplastic polymer bearing alkaline groupings, United States Patent No. 7973089 B2, 2011.

[23] J.-Y. Sanchez, F. Chabert, C. Iojoiu, J. Salomon, N.E. Kissi, Y. Piffard, M. Marechal, H. Galiano, R. Mercier, Extrusion: an environmentally friendly process for PEMFC membrane elaboration, Electrochim. Acta 53 (4) (2007) 1584–1594.

[24] Y. Molmeret, F. Chabert, N.E. Kissi, C. Iojoiu, R. Mercier, J.-Y. Sanchez, Toward extrusion of ionomers to process fuel cell membranes, Polymers 3 (3) (2011) 1126–1150.

[25] Y. Molmeret, F. Chabert, C. Iojoiu, N.E. Kissi, J.-.Y. Sanchez, Extruded proton exchange membranes based on sulfonated polyaromatic polymers for fuel cell application, in: Proceedings of the XV Annual Meeting International Congress on Rheology: The Society of Rheology, 80th Annual Meeting, Monterey, CA, 2008.

[26] M.T. Ponting, A. Hiltner, E. Baer, Polymer nanostructures by forced assembly: process, structure, and properties, Macromol. Symp. 294 (1) (2010) 19–32.

[27] M.T. Ponting, Gradient Multilayered Films & Confined Crystallization of Polymer Nanolayers by Forced Assembly Coextrusion (Ph.D. Dissertation), Department of Macromolecular Science & Engineering, Case Western Reserve University,

Cleveland, OH, 2010.
[28] M.T. Ponting, Y. Lin, J.K. Keum, A. Hiltner, E. Baer, Effect of substrate on the isothermal crystallization kinetics of confined poly(ε-caprolactone) nanolayers, Macromolecules 43 (20) (2010) 8619–8627.
[29] R.W. Baker, Vapor and gas separation by membranes, in: N.N. Li, A.G. Fane, W.S. Ho, T. Matsuura (Eds.), Advanced Membrane Technology and Applications, John Wiley & Sons, Inc, Hoboken, NJ, 2008, pp. 562–563.
[30] G.T. Offord, S.R. Armstrong, B.D. Freeman, E. Baer, A. Hiltner, J.S. Swinnea, D.R. Paul, Porosity enhancement in β nucleated isotactic polypropylene stretched films by thermal annealing, Polymer 54 (10) (2013) 2577–2589.
[31] G.T. Offord, S.R. Armstrong, B.D. Freeman, E. Baer, A. Hiltner, D.R. Paul, Influence of processing strategies on porosity and permeability of β nucleated isotactic polypropylene stretched films, Polymer 54 (11) (2013) 2796–2807.
[32] H.J. Oh, J.S. Park, S. Inceoglu, I. Villaluenga, J.L. Thelen, J. Xi, J.E. McGrath, D.R. Paul, Formation of disulfonated poly (arylene ether sulfone) thin film desalination membranes plasticized with poly (ethylene glycol) by solvent-free melt extrusion, Polymer 109 (2017) 106–114.
[33] H.J. Oh, J.E. McGrath, D.R. Paul, Kinetics of poly(ethylene glycol) extraction into water from plasticized disulfonated poly(arylene ether sulfone) desalination membranes prepared by solvent-free melt processing, J. Membr. Sci. 524 (2017) 257–265.
[34] H.J. Oh, Sulfonated Polysulfone Desalination Membranes by Melt Extrusion (Ph.D. Dissertation), Department of Chemical Engineering, The University of Texas at Austin, Austin, TX, 2015.
[35] J.E. Hensley, J.D. Way, S.F. Dec, K.D. Abney, The effects of thermal annealing on commercial Nafion membranes, J. Membr. Sci. 298 (2007) 190–201.
[36] C.E. Evans, R.D. Noble, S. Nazeri-Thompson, B. Nazeri, C.A. Koval, Role of conditioning on water uptake and hydraulic permeability of Nafion membranes, J. Membr. Sci. 279 (2006) 521–528.
[37] N.P. Berezina, S.V. Timofeev, N.A. Kononenko, Effect of conditioning techniques of perfluorinated sulphocationic membranes on their hydrophylic and electrotransport properties, J. Membr. Sci. 209 (2002) 509–518.
[38] L. Yang, F. Heatley, T.G. Blease, R.I.G. Thompson, A study of the mechanism of the oxidative thermal degradation of poly(ethylene oxide) and poly(propylene oxide) using ^{1}H and ^{13}C NMR, Eur. Polym. J. 32 (5) (1996) 535–547.
[39] G.M. Geise, H.-S. Lee, D.J. Miller, B.D. Freeman, J.E. McGrath, D.R. Paul, Water purification by membranes: the role of polymer science, J. Polym. Sci. Part B: Polym. Phys. 48 (15) (2010) 1685–1718.
[40] A.C. Sagle, E.M. Van Wagner, H. Ju, B.D. McCloskey, B.D. Freeman, M.M. Sharma, PEG-coated reverse osmosis membranes: desalination properties and fouling resistance, J. Membr. Sci. 340 (1–2) (2009) 92–108.
[41] W. Xie, Preparation and Characterization of Disulfonated Polysulfone Films and Polyamide Thin Film Composite Membranes for Desalination (Ph.D. Dissertation), Department of Chemical Engineering, The University of Texas at Austin, Austin, TX, 2011.
[42] D.R. Paul, Reformulation of the solution-diffusion theory of reverse osmosis, J. Membr. Sci. 241 (2004) 371–386.
[43] D.R. Paul, Relation between hydraulic permeability and diffusion in homogeneous swollen membranes, J. Polym. Sci.: Polym. Phys. Ed. 11 (1973) 289–296.
[44] J.G. Wijmans, R.W. Baker, The solution-diffusion model: a review, J. Membr. Sci. 107 (1995) 1–21.
[45] H. Yasuda, C.E. Lamaze, A. Peterlin, Diffusive and hydraulic permeabilities of water in water-swollen polymer membranes, J. Polym. Sci. Part A-2: Polym. Phys. 9 (6) (1971) 1117–1131.
[46] P.J. Flory, Thermodynamics of high polymer solutions, J. Chem. Phys. 10 (1942) 51–61.
[47] M.L. Huggins, Solutions of long chain compounds, J. Chem. Phys. 9 (5) (1941) 440.
[48] G.M. Geise, Water and Salt Transport Structure/Property Relationship in Polymer Membranes for Desalination and Power Generation Applications (Ph.D. Dissertation), Department of Chemical Engineering, University of Texas at Austin, Austin, TX, 2012.
[49] H. Yasuda, C.E. Lamaze, L.D. Ikenberry, Permeability of solutes through hydrated polymer membranes. Part I. Diffusion of sodium chloride, Die Makromol. Chem. 18 (1) (1968) 19–35.
[50] H. Ju, A.C. Sagle, B.D. Freeman, J.I. Mardel, A.J. Hill, Characterization of sodium chloride and water transport in crosslinked poly(ethylene oxide) hydrogels, J. Membr. Sci. 358 (1–2) (2010) 131–141.
[51] W. Xie, H. Ju, G.M. Geise, B.D. Freeman, J.I. Mardel, A.J. Hill, J.E. McGrath, Effect of free volume on water and salt transport properties in directly copolymerized disulfonated poly(arylene ether sulfone) random copolymers, Macromolecules 44 (11) (2011) 4428–4438.
[52] G.M. Geise, C.L. Willis, C.M. Doherty, A.J. Hill, T.J. Bastow, J. Ford, K.I. Winey, B.D. Freeman, D.R. Paul, Characterization of aluminum-neutralized sulfonated styrenic pentablock copolymer films, Ind. Eng. Chem. Res. 52 (3) (2013) 1056–1068.
[53] P.R. Bevington, D.K. Robinson, Data Reduction and Error Analysis for the Physical Sciences (146-148, 194-217), McGraw-Hill Eduation, New York City, NY, 2003, pp. 43–44.
[54] Y. Ma, F. Shi, J. Ma, M. Wu, J. Zhang, C. Gao, Effect of PEG additive on the morphology and performance of polysulfone ultrafiltration membranes, Desalination 272 (1–3) (2011) 51–58.
[55] Z.-L. Xu, F.A. Qusay, Effect of polyethylene glycol molecular weights and concentrations on polyethersulfone hollow fiber ultrafiltration membranes, J. Appl. Polym. Sci. 91 (5) (2004) 3398–3407.
[56] B. Chakrabarty, A.K. Ghoshal, M.K. Purkair, Effect of molecular weight of PEG on membrane morphology and transport properties, J. Membr. Sci. 309 (1–2) (2008) 209–221.
[57] A. Idris, N.M. Zain, M.Y. Noordin, Synthesis, characterization and performance of asymmetric polyethersulfone (PES) ultrafiltration membranes with polyethylene glycol of different molecular weights as additives, Desalination 207 (2007) 324–339.
[58] J.-H. Kim, K.-H. Lee, Effect of PEG additive on membrane formation by phase inversion, J. Membr. Sci. 138 (2) (1998) 153–163.
[59] A.K. Holda, F.J. Vankelecom, Integrally skinned PSf-based SRNF-membranes prepared via phase inversion—Part B: influence of low molecular weight additives, J. Membr. Sci. 450 (15) (2014) 499–511.
[60] A.F. Ismail, A.R. Hassan, Effect of additive contents on the performances and structural properties of asymmetric polyethersulfone (PES) nanofiltration membranes, Sep. Purif. Technol. 55 (1) (2007) 98–109.
[61] W.-L. Chou, D.-G. Yu, M.-C. Yang, C.-H. Jou, Effect of molecular weight and concentration of PEG additives on morphology and permeation performance of cellulose acetate hollow fibers, Sep. Purif. Technol. 57 (2) (2007) 209–219.
[62] J.-F. Li, Z.-L. Xu, H. Yang, C.-P. Feng, J.-H. Shi, Hydrophilic microporous PES membranes prepared by PES/PEG/DMAc casting solutions, J. Appl. Polym. Sci. 107 (6) (2007) 4100–4108.
[63] B. Chakrabarty, A.K. Ghoshal, M.K. Purkait, Effect of molecular weight of PEG on membrane morphology and transport properties, J. Membr. Sci. 309 (1–2) (2008) 209–221.
[64] G.M. Geise, H.B. Park, A.C. Sagle, B.D. Freeman, J.E. McGrath, Water permeability and water/salt selectivity tradeoff in polymers for desalination, J. Membr. Sci. 369 (2011) 130–138.
[65] D.R. Paul, The role of membrane pressure in reverse osmosis, J. Appl. Polym. Sci. 16 (1972) 771–782.